

# Merger rates of dark matter haloes from merger trees in the extended Press-Schechter theory

Nicos Hiotelis\* †

*1st Experimental Lyceum of Athens, Ipitou 15, Plaka, 10557, Athens, Greece, E-mail: hiotelis@ipta.demokritos.gr*

Accepted ..... Received .....; in original form .....

## ABSTRACT

We construct merger trees based on the extended Press-Schechter theory (EPS) in order to study the merger rates of dark matter haloes over a range of present day mass ( $10^{10}M_{\odot} \leq M_0 \leq 10^{15}M_{\odot}$ ), progenitor mass ( $5 \times 10^{-3} \leq \xi \leq 1$ ) and redshift ( $0 \leq z \leq 3$ ). We used the first crossing distribution of a moving barrier of the form  $B(S, z) = p(z) + q(z)S^{\gamma}$ , proposed by Sheth & Tormen, to take into account the ellipsoidal nature of collapse. We find that the mean merger rate per halo  $B_m/n$  depends on the halo mass  $M$  as  $M^{0.2}$  and on the redshift as  $(d\delta_c(z)/dz)^{1.1}$ . Our results are in agreement with the predictions of N-body simulations and this shows the ability of merger-trees based on EPS theory to follow with a satisfactory agreement the results of N-body simulations and the evolution of structures in a hierarchical Universe.

**Key words:** cosmology: theory – dark matter, galaxies: haloes – structure – formation, methods: analytical

## 1 INTRODUCTION

Although numerical experiments are the most powerful methods to study the formation of structures, the development of analytical or semi-numerical methods is very important, since they help to improve our understanding of the physical processes during the formation.

A class of analytical methods is that based on the ideas of Press & Schechter (1974) and on their extensions (Bond et al. 1991, Lacey & Cole 1993):

The linear overdensity computed at a given point of an initial snapshot of the Universe fluctuates when the smoothing scale decreases. This fluctuation is a Markovian process when the smoothing is performed using a top-hat window in Fourier space. For any value of the smoothing scale  $R$  the overdensity field is assumed to be Gaussian. The mass  $M$  contained in a given scale  $R$  depends on the window function used. For a top-hat window the relation is:

$M = \frac{4}{3}\rho_{b,i} R^3 = \frac{\Omega_{m,i}H_i^2}{2G}R^3$ , where  $\rho_{b,i}$  and  $\Omega_{m,i}$  are the values of the mean density and the density parameter of the Universe,  $G$  is the gravitational constant and  $H_i$  is the Hubble's constant. The index  $i$  indicates that all the above values are calculated at the initial snapshot. Mass dispersion  $\sigma^2$  at scale  $R$  is a function of mass  $M$  and is usually denoted by  $S$ , that is  $S(M) \equiv \sigma^2[R(M)]$ . Let the random walk of the overdensity cross for first time a given barrier

$B(S, z)$  at some value  $S_0$  of  $S$ . The mass element associated with the random walk is considered to belong to a halo of mass  $M_0 = S^{-1}(S_0)$  at the epoch with redshift  $z$ . The distribution of haloes, at some epoch  $z$ , is related to the first crossing distributions, by the random walks, of the barrier that corresponds to epoch  $z$ .

The simplest form of the barrier comes from the spherical model. It is well known that in an Einstein-de Sitter Universe, a spherical overdensity collapses at  $z$  if the linear extrapolation of its value up to the present exceeds  $\delta_{sc} \approx 1.686$ , and this value provides a first reasonable choice for the barrier. The involved quantities (density overdensities, dispersion) are usually extrapolated to the present epoch and thus the barrier in the spherical collapse model is written in the form  $B(S, z) = 1.686/D(z)$ , where  $D(z)$  is the growth factor derived by the linear theory with  $D(z=0) = 1$ . The form of the spherical barrier permits the analytical evaluation of the first crossing distribution  $f(S)$ .

Despite the simplicity of the spherical model, its results agree relatively well with the results of N-body simulations (e.g. White, Efstathiou & Frenk 1993; Lacey & Cole 1994; Gelb & Bertschinger 1994; Bond & Myers 1996). Deviations appear in the resulting mass functions at both high and low masses. Sheth & Tormen (1999) consider a barrier of the form  $B(S, z) = p(z) + q(z)S^{\gamma}$  with  $p(z) = 0.840\delta_c(z)$ ,  $q(z) = 0.505\delta_c(z)^{-0.23}$ , where  $\delta_c(z) = 1.686/D(z)$  and  $\gamma = 0.615$ , in order to describe the ellipsoidal form of collapse. The first crossing distribution  $f(S, z)$  that results from the ellipsoidal model works better than the spherical one. For example, Yahagi et al. (2004) showed that the multiplicity function

\* E-mail: hiotelis@ipta.demokritos.gr

† Present address: Lysimahias 66, Neos Kosmos, Athens, 11744 Greece

resulting from N-body simulations is far from the predictions of spherical model while it shows an excellent agreement with the results of the ellipsoidal model. On the other hand, Lin et al. (2003) compared the distribution of formation times of haloes formed in N-body simulations with the formation times of haloes formed in terms of the spherical collapse model. They found that N-body simulations give smaller formation times. Hiotelis & del Popolo (2006) used merger trees to show that the ellipsoidal collapse model leads to formation times that are shifted to smaller values relative to the spherical collapse model. Thus, a better agreement with the predictions of N-body simulations is achieved. The distributions of formation times are studied in more detail by other authors (Giocoli et al. 2007). We note that in the cases of a barrier with  $\gamma = 1$ , or  $\gamma = 0.5$ , the corresponding first crossing distribution can be found analytically (e.g. Mahmood & Rajesh 2005). For the above non-linear barrier, Sheth & Tormen (2002) proposed an analytical expression. It is shown that this analytical expression approximates well the exact expression found as a numerical solution of an integral equation (Zhang & Hui 2008).

The constrained first crossing distribution is given by the relation:

$$f(S, z/S, z_0) dS = \frac{1}{\sqrt{2\pi}} \frac{|T(S, z/S_0, z_0)|}{(\Delta S)^{3/2}} \exp\left[-\frac{(\Delta B)^2}{2\Delta S}\right] dS \quad (1)$$

where  $\Delta S = S - S_0$ ,  $\Delta B = B(S, z) - B(S_0, z_0)$  and the function  $T$  is given by:

$$T(S, z/S_0, z_0) = B(S, z) - B(S_0, z_0) + \sum_{n=1}^5 \frac{[S_0 - S]^n}{n!} \frac{\partial^n}{\partial S^n} B(S, z) \quad (2)$$

Given that a mass element is a part of a halo of mass  $M_0$  at redshift  $z_0$  the probability that at higher redshift  $z$  this mass element was a part of a smaller halo  $M$  is given by Eq.(1). The unconstrained expression,  $f(S, z)$ , results by setting  $S_0 = B(S_0, z_0) = 0$ . The analytical expression is very useful since it allows the construction of merger trees. The purpose of this paper is:

- (i) To construct merger trees able to give merger rates of dark matter haloes.
- (ii) To compare these merger rates with those predicted by the results of N-body simulations.
- (iii) To extend the calculations to scales that are not accessible by numerical simulations and finally,
- (iv) to study the role of some of the main parameters involved.

In Sect. 2 we give a brief description of the tree code used. Then, the definition of merger rates is presented and the analytical formulae, predicted by other authors from the results of N-body simulations, are given. In Sect. 3 we present our results.

## 2 TREE CONSTRUCTION, DEFINITIONS OF HALO MERGER RATES FITTING FORMULAE

### 2.1 Tree construction

Merger-trees used in this paper are constructed using Eq.(1). Let us assume a descendant halo of mass  $M_d$  at redshift  $z_d$ . We study its past by the following procedure: A new larger redshift  $z_p$  is chosen. This is done by solving for  $z_p$  the equation  $\delta_c(z_p) - \delta_c(z_d) = D$ , where  $D$  is a constant (one of the parameters of the algorithm). Then, a value  $S_p$  is chosen from the distribution (1). The mass of the progenitor is  $M_p = S^{-1}(S_p)$ . This progenitor is accepted if its mass is larger than a lower limit  $M_{min}$  and smaller than the mass left to be resolved. If  $M_p$  is less than  $M_{min}$  then  $M_p$  is added to a sum that is named  $M_{accr}$ . The mass left to be resolved is, at the choice of the  $k$ -th progenitor,  $M_{left} = M_d - \sum_{l=1}^{k-1} M_{p,l} - M_{accr}$ . If  $M_{left}$  is larger than  $M_{min}$  we proceed to the selection of a next progenitor, while if  $M_{left}$  is smaller than  $M_{min}$  we proceed to the next redshift. It is obvious that in such construction, the number of progenitors can be larger than two, despite the original assumption of Lacey & Cole (1993), and this leads to a better representation of the distribution of progenitors. Our algorithm is based on the ‘‘N-branch’’ idea of Somerville & Kollat (1999), but extended in order to incorporate aspects of the ellipsoidal collapse results. A complete description of the tree construction is given in Hiotelis & del Popolo (2006). The comparisons between the predictions of the tree and analytical predictions of the distribution of the number of progenitors show that the tree method is reliable in following the evolution of structures. Various tree-construction algorithms have been presented in the literature (Cole 1991; Kauffmann & White 1993; Sheth & Lemson 1999; Cole et al. 2000; Neinstein & Dekel 2008). The accuracy of these algorithms is usually against simplicity. For example, the algorithm of Neinstein & Dekel (2008) requires the solution of several differential equations with nontrivial boundary conditions.

### 2.2 Definition of merger-rates

We examine one descendant halo from a sample of  $N_d$  haloes with masses in the range  $M_d, M_d + dM_d$  present at redshift  $z_d$ . For a single halo the procedure is as follows: Let  $M_{p,1}, M_{p,2} \dots M_{p,k}$  be the masses of its  $k$  progenitors at redshift  $z_p > z_d$ . For matter of simplicity we assume that the most massive progenitor is  $M_{p,1}$ . We define  $\xi_i = M_{p,i}/M_{p,1}$  for  $i \geq 2$  and we assume that the descendant halo is formed by the following procedure: During the interval  $dz = z_p - z_d$  every one of the progenitors with  $i \geq 2$  merge with the most massive progenitor  $i = 1$  and form the descendant halo we examine. We repeat the above procedure for all haloes in the range  $M_d, M_d + dM_d$  found in a volume  $V$  of the Universe. Then, we find the number denoted by  $N$  of all progenitors with  $\xi_i, i \geq 2$  in the range  $(\xi, \xi + d\xi)$  and we calculate the ratio  $N/(V dz dM_d d\xi)$ . We define the merger rate  $B_m$  as follows:

$$B_m(M_d, \xi, z_p : z_d) = \frac{N}{V dz dM_d d\xi} \quad (3)$$

Let the number density of haloes with masses in the range  $M_d, M_d + dM_d$  at  $z_d$  be  $n(M_d, z_d) = \frac{N_d(M_d, z_d)}{V dM_d}$ . The ratio  $B_m/n = N/(N_d dz d\xi)$  measures the mean number of mergers per halo, per unit redshift, for descendant haloes in the range  $M_d, M_d + dM_d$  with progenitor mass ratio  $\xi$ .

We note that the definition of mean merger rate is exactly the same as in Fakhouri & Ma (2008) (FM08 hereafter). We also use the assumption that all progenitors merge with the most massive one (see FM08 for a discussion of this assumption.)

Lacey & Cole (1993) showed that in the spherical model the transition rate is given by:

$$r(M \rightarrow M_d/z_d) dM_d = \left(\frac{2}{\pi}\right)^{1/2} \left[\frac{d\delta_c(z)}{dz}\right]_{z=z_d} \times \frac{1}{\sigma^2(M_d)} \left[1 - \frac{\sigma^2(M_d)}{\sigma^2(M)}\right]^{-3/2} \left[\frac{d\sigma(M)}{dM}\right]_{M=M_d} \times \exp\left[-\frac{\delta_c^2(t)}{2} \left(\frac{1}{\sigma^2(M_d)} - \frac{1}{\sigma^2(M)}\right)\right] dM_d \quad (4)$$

This provides the fraction of the mass belonging to haloes of mass  $M$  that merge instantaneously to form haloes of mass in the range  $M_d, M_d + dM_d$  at  $z_d$ . The product  $r \cdot f_{sc}(M, z_d) dM$ , where  $f_{sc}(M, z)$  is the unconditional first crossing distribution for the spherical model, gives the above fraction of mass as a fraction of the total mass of the Universe and successively multiplying by  $(\rho_b/M) \cdot V$  the number of those haloes is found. Then, by dividing by  $(\rho_b/M_d) \cdot V \cdot f_{sc}(M_d, z_d) dM_d$  (that equals to the number of the descendant haloes) we find:

$$\frac{N}{N_d dz} = \sqrt{\frac{2}{\pi}} \frac{M_d}{M} \frac{1}{\sigma^2(M)} \frac{d\sigma(M)}{dM} \left[\frac{d\delta_c(z)}{dz}\right]_{z=z_d} \times \left[1 - \frac{\sigma^2(M_d)}{\sigma^2(M)}\right]^{-3/2} dM \quad (5)$$

Assuming a binary merge, where  $\xi$  is the ratio of the small progenitor to the large one ( $\xi = (M_d - M)/M$ ), using  $dM = \frac{M}{M_d} d\xi$  and substituting in (5) we have the final expression for the binary spherical case, that is:

$$\frac{B_m}{n} = \frac{N}{N_d dz d\xi} = \sqrt{\frac{2}{\pi}} \frac{M}{\sigma^2(M)} \frac{d\sigma(M)}{dM} \left[\frac{d\delta_c(z)}{dz}\right]_{z=z_d} \times \left[1 - \frac{\sigma^2(M_d)}{\sigma^2(M)}\right]^{-3/2} \quad (6)$$

### 2.3 Fitting formulae

FM08 analyzed the results of the Millennium simulation of Springel et al. (2005). Stewart et al. (2008), (SBBW08 hereafter), used their high-resolution N-body simulations to study the merger rates of dark matter haloes. Fitting formulae proposed by the above authors are separable in the three variables, mass  $M_d$ , progenitor ratio  $\xi$  and redshift  $z$ . These formulae are of the form:

$$\frac{B(M_d, \xi, z_p : z_d)}{n(M_d, z)} = A \cdot F(M_d) G(\xi) H(z) \quad (7)$$

FM08 proposed  $A = 0.0289, F(M_d) = \left(\frac{M_d}{M}\right)^{a_1}, G(\xi) = \xi^{a_2} \exp\left[\left(\frac{\xi}{\tilde{\xi}}\right)^{a_3}\right], H(z) = \left(\frac{d\delta_c}{dz}\right)_{z=z_d}^{a_4}$ . where the values of the parameters are  $\tilde{M} = 1.2 \times 10^{12} M_\odot, A = 0.0289, \tilde{\xi} = 0.098, a_1 = 0.083, a_2 = -2.01, a_3 = 0.409, a_4 = 0.371$ .

On the other hand, SBBW08 proposed:  $A = 0.27, F(M_d) = \left(\frac{M_d}{M}\right)^{b_1}, G(\xi) = (1 - \xi)^{b_3 - 1} [(b_3 - b_2)\xi + b_2]/\xi^{b_2 + 1}, H(z) = \left(\frac{d\delta_c}{dz}\right)_{z=z_d}^{b_4}$  where  $\tilde{M} = 10^{12} h^{-1} M_\odot, b_1 = 0.15, b_2 = 0.5, b_3 = 1.3, b_4 = 2$ .

Note that the formulae proposed by the above authors show some significant differences. First, the dependence on redshift  $z$  differs in the above two formulae. Although the quantity  $d\delta_c/dz$  does not vary significantly with redshift, the exponents  $a_4$  and  $b_4$  can cause significant differences in the merger rates. Second, exponents  $a_1$  and  $b_1$  that define the dependence on the mass are quite different. In the approximation of FM08 mean merger rates are practically independent on mass.

Additionally, the above formulae show significant differences in their slope at small and large values of  $\xi$ . The logarithmic slope of  $G$ ,  $d \ln G(\xi)/d \ln \xi$ , at  $\xi = 0$  is  $a_2 = -2.01$  for the FM08 model, and  $-b_2 - 1 = -1.5$  for the SBBW08 model. For  $\xi \rightarrow 1$  the above logarithmic slope is  $a_2 + a_3(1/\tilde{\xi})^{a_3} = -0.952$  for the FM08 model and it tends to  $-\infty$  in the formula of SBBW08.

Therefore, it is interesting to study merger rates predicted by merger-trees and to compare their characteristics with those of the above fitting formulae.

### 3 RESULTS

We used a flat model for the Universe with  $\Omega_{m,0} = 0.3$  and  $\Omega_{\Lambda,0} = 0.7$  and a power spectrum proposed by Smith et al. (1998) given by:

$$P(k) = \frac{A k^n}{[1 + a_1 k^{1/2} + a_2 k + a_3 k^{3/2} + a_4 k^2]^b} \quad (8)$$

The values for the parameters are:  $n = 1, a_1 = -1.5598, a_2 = 47.986, a_3 = 117.77, a_4 = 321.92$  and  $b = 1.8606$ . Smoothed fields are calculated using the top-hat window function. The constant  $A$  of proportionality, is found using the procedure of normalization. We used two different values for the normalization namely  $\sigma_8 \equiv \sigma(R = 8h^{-1} \text{Mpc}) = 0.9$  and  $1$  respectively. We also use a system of units where  $M_{\text{unit}} = 10^{12} h^{-1} M_\odot, R_{\text{unit}} = h^{-1} \text{Mpc}$  and  $t_{\text{unit}} = 1.515 \times 10^7 h^{-1} \text{years}$ . In this system of units,  $H_0/H_{\text{unit}} = 1.5276$ . We performed a large number of tree realizations in order to study merger rates. First, we found that good fits are achieved by both of the above formulae but for different values of the parameters than those proposed by the above authors. We found that merger rates depend on the mass of the descendant halo as  $M_d^{0.2}$  and on the redshift as  $[d\delta_c/dz]^{1.1}$ . So, in the comparisons that follow, the formulae of Eq. 7 are used with  $a_1 = b_1 = 0.2, a_4 = b_4 = 1.1$ . Additionally, in the formula of SBBW08, we use the value of  $b_2 = 0.7$  instead of  $b_2 = 0.5$ .

In Fig.1, comparisons between the predictions of merger trees and those of formulae given by Eq. 7 are shown. The power spectrum used is that given by Eq. 8 for  $\sigma_8 = 1$ . Details are given in the caption of the figure. We note a very

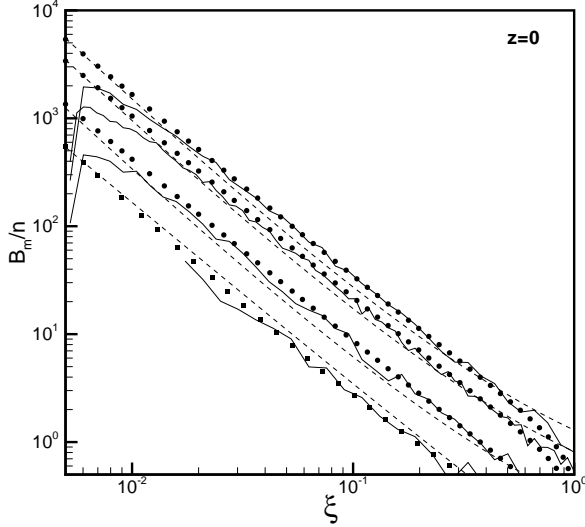


**Figure 1.** From top to bottom, dots correspond to the mean present merger rates ( $z = 0$ ) for haloes with present day masses  $10^{15} h^{-1} M_{\odot}$ ,  $10^{14} h^{-1} M_{\odot}$ ,  $10^{12} h^{-1} M_{\odot}$  and  $10^{10} h^{-1} M_{\odot}$  respectively, predicted by the formula proposed by FM08 for  $a_1 = 0.2$  and  $a_4 = 1.1$ . Dashed lines are predicted by the formula proposed by SBBW08 for  $b_1 = 0.2$  and  $b_2 = 0.7$ . Solid lines are the predictions of merger trees described in the text by Eq.(3) for  $z_d = 0$  and  $z_p = 0.0556$ . We used a sample of 10000 present-day haloes for each of the three cases and we evolved the system by a single time-step for  $D = 0.05$ . The minimum mass  $M_{min}$  in every case equals to 0.005 times  $M_d$ .

good agreement but also a rapid fall of the predictions of merger trees for small values of  $\xi$ . We will show below that this is a matter of resolution that depends on the value of  $M_{min}$ .

The predictions of this figure are just after one time step of the tree algorithm. For a higher redshift  $z_1$  one has to use one of the two alternatives: To start with a sample of haloes at  $z_1$  and after a single time step to move to a new redshift  $z_{p1}$ , to calculate the merger rates, or to start with a sample of haloes at the present epoch  $z = 0$  and to calculate merger rates after a number of time steps when the redshift has a desirable value. Obviously, the second approach tests the ability of the merger tree to follow the time evolution of structures and it is close to the nature of N-body simulations. This approach is followed in our calculations.

Fig.2 shows merger rates predicted by a merger tree, started at  $z = 0$ , after 22 time steps, for  $D = 0.05$  and  $\sigma_8 = 1$ . Redshifts are  $z_d = 0.979$ ,  $z_p = 1.021$ . The sample of haloes at  $z = 0$  consists of 36500 haloes each with mass  $M_0 = 10^{14} h^{-1} M_{\odot}$ . The number of haloes in the range  $1.5 - 2.5 \times 10^{13} h^{-1} M_{\odot}$  at  $z_d$  is  $N_p = 19241$  and  $N_d = 15465$ . In the range  $4.5 - 5.5 \times 10^{13} h^{-1} M_{\odot}$  there are  $N_p = 7587$  and  $N_d = 4961$  haloes. Finally, in the range  $6.5 - 7.5 \times 10^{13} h^{-1} M_{\odot}$  there are  $N_p = 5803$  and  $N_d = 3330$  haloes. The resolution mass,  $M_{min}$  used is  $5 \times 10^{11} h^{-1} M_{\odot}$ . For  $z = 1$  long dashes show the formula of SBBW08, dots the formula of FM08 and small dashes the prediction of the binary spherical model given by Eq. 6. In the following we examine the role of some of the

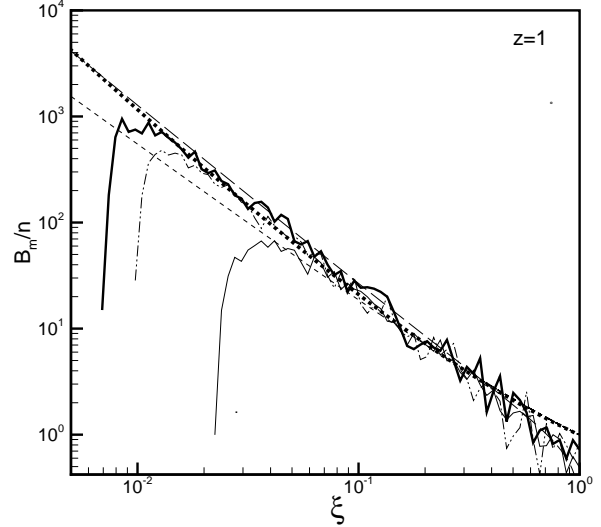


**Figure 2.** Thin solid line, dashed-dot-dot line and thick solid line show the mean merger rate at  $z \approx 1$  for haloes with masses in the range  $M_1 = 1.5 - 2.5 \times 10^{13} h^{-1} M_{\odot}$ ,  $M_2 = 4.5 - 5.5 \times 10^{13} h^{-1} M_{\odot}$  and  $M_3 = 6.5 - 7.5 \times 10^{13} h^{-1} M_{\odot}$ , respectively. The merger tree used started at  $z = 0$  with  $D = 0.05$  for a sample of 36500 haloes each of mass  $10^{14} h^{-1} M_{\odot}$ . After 22 time steps the redshifts are  $z_d = 0.979$ ,  $z_p = 1.021$ . The resolution mass is  $M_{min} = 5 \times 10^{11} h^{-1} M_{\odot}$ . Long dashes, big dots and small dashes are the results from the formulae of SBBW08, FM08 and the binary spherical model for  $M_d = 5 \times 10^{13} h^{-1} M_{\odot}$  at  $z = 1$ .

large number- of the parameters involved in the construction of merger trees. These are:

- (i) the resolution mass  $M_{min}$
- (ii) the step in redshift, defined by the parameter  $D$
- (iii) the value of  $\sigma_8$  and
- (iv) the number of realizations, that is the number of haloes at  $z = 0$ .

Resolution mass  $M_{min}$  is a crucial parameter. A sample of present day haloes of mass  $M_0$  is analyzed to smaller and smaller haloes as the redshift becomes higher. Let  $M_d$  be the mass of a descendant halo at some high redshift,  $M_1$  its largest progenitor and  $M_2$  another progenitor. Obviously,  $M_1 \leq M_d - M_{min}$  and  $M_2 \geq M_{min}$ . Thus  $\xi = \frac{M_2}{M_1} \geq \frac{M_{min}}{M_d - M_{min}} \equiv \xi_{min}$  and consequently  $\xi_{min}$  and  $M_{min}$  are related by  $M_{min} = M_d(1 + \xi_{min}^{-1})^{-1}$ . Since at high redshifts  $M_d$  is significantly smaller than  $M_0$ , the condition for the merger rate curves to extend to the left up to values as small as  $\xi_{min}$  is  $M_{min} \ll M_0(1 + \xi_{min}^{-1})^{-1}$ . We found that for decreasing  $M_{min}$  the value  $\xi$ , at which the merger rates curves show their rapid fall, moves to the left. Thus, this rapid fall seen in Figs 1 and 2 is clearly a matter of resolution.

On the other hand, the results do not seem to be sensitive to the values of the step in redshift  $z$ . This step depends on the parameter  $D$  described in section 2.1. We examined cases, for  $D=0.025$ ,  $D=0.05$  and  $D=0.1$ . We found that the results are the same.

Fig.3 shows the role of the above two parameters. It presents

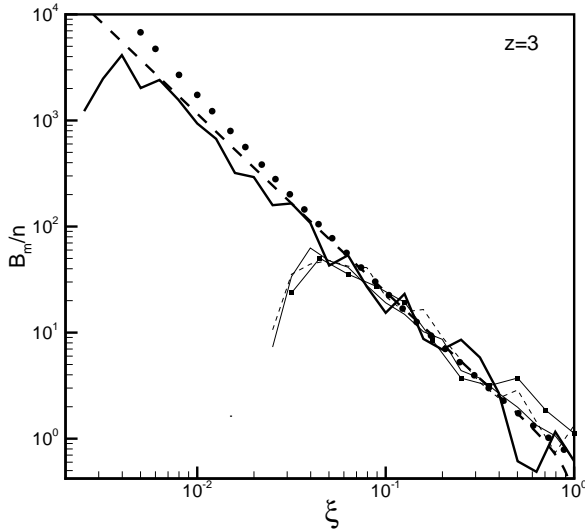


**Figure 3.** Merger rates for descendant haloes with masses in the range  $1.5 - 2.5 \times 10^{13} h^{-1} M_{\odot}$ , for an initial sample of 10000 haloes each with mass  $10^{14} h^{-1} M_{\odot}$  after 72 steps (thin solid line), after 144 steps (thin solid line with large dots) and after 36 steps (line with thin and small dashes). These three lines correspond to about the same redshift ( $z=3$ ), and to the same resolution mass  $M_{min} = 5 \times 10^{11} h^{-1} M_{\odot}$ . Thick solid line is the prediction for smaller minimum mass,  $M_{min} = 5 \times 10^{10} h^{-1} M_{\odot}$ . Big dots are the predictions of FM08, while large thick dashes, the predictions of SBBW08.

merger rates, for descendant haloes with masses in the range  $1.5 - 2.5 \times 10^{13} h^{-1} M_{\odot}$ , for an initial sample of 10000 haloes, each with mass  $10^{14} h^{-1} M_{\odot}$ , after 72 steps (thin solid line), after 144 steps (thin solid line with large dots) and after 36 steps (line with thin and small dashes). All lines correspond to about the same redshift ( $z=3$ ), since we used different values for the time step parameter,  $D = 0.05$ ,  $D = 0.025$  and  $D = 0.1$ , respectively. The corresponding redshifts are ( $z_d = 2.971, z_p = 3.011$ ), ( $z_d = 3.005, z_p = 3.025$ ), ( $z_d = 2.921, z_p = 3.000$ ), respectively. We see that the resulting merger rates are similar, although the values of  $dz$  used in Eq. 3 differ,  $dz \approx 0.02, 0.04, 0.08$ .

In the same figure the thick solid line is the prediction for a resolution mass an order of magnitude smaller, namely  $M_{min} = 5 \times 10^{10} h^{-1} M_{\odot}$  and shows the above described role of  $M_{min}$ . Finally, big dots and thick dashes are the predictions of FM08 and SBBW08, respectively, for values of the parameters given above. All calculations in Fig.3 are for 10000 present day haloes and for  $\sigma_8 = 1$ . The above described role of the two parameters is the same for the range of present day masses,  $10^{10} M_{\odot} \leq M_0 \leq 10^{15} M_{\odot}$ , we examined. We note that small values of  $M_{min}$  lead to large numbers of haloes at the past. For example, 10000 present day haloes with mass  $10^{15} M_{\odot}$  have for  $M_{min} = 5 \times 10^{12} M_{\odot}$ , about  $1.2 \times 10^5$  progenitors at  $z \approx 3$ . For the minimum value of  $M_{min}$  that we have used, that is  $M_{min} = 5 \times 10^{10} M_{\odot}$  and corresponds to a resolution  $1 : 20000$ , at the same redshift, the number of progenitors is larger than  $1.5 \times 10^6$ . Thus, tree construction becomes a computing time consuming procedure.

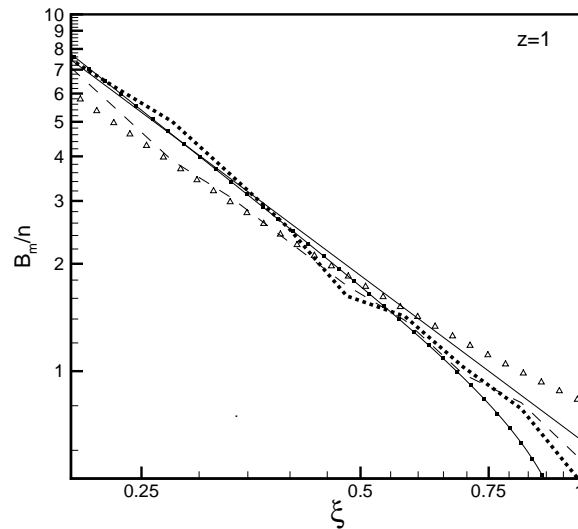


**Figure 4.** Merger rates for descendant haloes with masses in the range  $1.5 - 2.5 \times 10^{13} h^{-1} M_{\odot}$  at  $z = 1$ . Dots are the predictions for the power spectrum normalized to  $\sigma_8 = 1$ , while dashes correspond to  $\sigma_8 = 0.9$ . Solid line shows a law  $\propto \xi^{-1.52}$  for comparison. Deltas correspond to the model of FM08 while solid line with black squares to the model of SBBW08.

Major mergers seem to play an important role in the formation of dark matter haloes. N-body simulations show that haloes which experienced a recent major merger event, appear to have lower concentrations and steeper inner density profiles (e.g. Ascasibar et al. 2003, Tasitsiomi et al. 2004) as well as larger values of spin parameters (Gardner 2001, Peirani et al. 2004). This last result is also supported by semi-numerical results (e.g. Vitvitska et al. 2002, Hiotelis 2008). Thus, it is interesting to study in more detail the behavior of merger rates curves at large values of  $\xi$ . This demands smooth curves and consequently large number of haloes. So, in Fig.4 we present an example of the role of the last two of the parameters we examined. These parameters are the number of present day haloes and the value of  $\sigma_8$ . All curves of this figure correspond to  $z = 1$ . Dots are the predictions for a set of 36500 present day haloes each with mass  $M_0 = 10^{14} h^{-1} M_{\odot}$  for a power spectrum with  $\sigma_8 = 1$  and for descendant haloes in the range  $1.5 \times 10^{13} h^{-1} M_{\odot} - 2.5 \times 10^{13} h^{-1} M_{\odot}$ . At  $z = 1$ , there are  $N_p = 19241$  and  $N_d = 15456$  haloes. Dashes are the predictions for a set of  $1.5 \times 10^5$  present day haloes of the same mass for  $\sigma_8 = 0.9$  and for the above range of mass of the descendant haloes. At  $z = 1$ , there are  $N_p = 104873$  and  $N_d = 70276$  haloes. Solid line shows a law  $\propto \xi^{-1.52}$  for comparison. Deltas are the predictions of the fitting formula of FM08 and finally, the solid line with big dots shows the predictions of SBBW08. Fig.5 is similar to Fig.4 but for  $z = 3$  and for descendant haloes in the range  $5 \times 10^{12} h^{-1} M_{\odot} - 10^{13} h^{-1} M_{\odot}$ . There are  $N_p = 26610$  and  $N_d = 24540$  for the tree corresponding to the dashed line while there are  $N_p = 129074$  and  $N_d = 109678$  for the tree corresponding to dots. It is clear from the above two figures, that - at the level of accuracy of the calculations

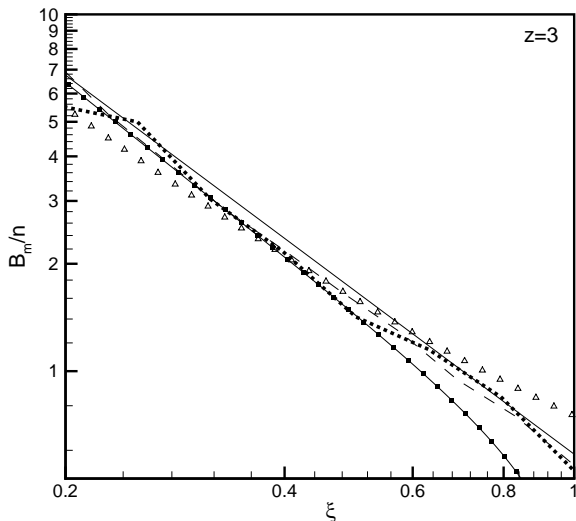


**Figure 5.** As in Fig.4 but for  $z=3$ .

of this paper - no differences can be detected due to the difference between 0.9 and 1.0 of the values of  $\sigma_8$ . Larger number of present day haloes leads, obviously, to smoother curves but they cause no difference in the overall shape.

#### 4 DISCUSSION

The above study of merger rates that are predicted by merger trees based on the extended PS theory using the ellipsoidal collapse model, leads to the following conclusions that hold for haloes in the range of mass  $10^{12}h^{-1}M_\odot - 10^{15}h^{-1}M_\odot$  and for redshift  $0 \leq z \leq 3$ .

(i) Merger rates depend on the mass of the descendant halo as  $\sim M^n$  with  $n=0.2$ . This dependence is in practice indistinguishable from the value  $n = 0.15$  proposed from SBBW08 but is far from the value of  $n = 0.083$  proposed by FM08.

(ii) We found that merger rates depend on the redshift through the quantity  $[\delta_c(z)/dz]^l$ , where  $l = 1.1$ . This value of the exponent  $l$  is close to the value predicted by the binary spherical case (see Eq.6) and between the values 0.371 and 2 proposed by FM08 and SBBW08, respectively.

(iii) The results of merger trees are in better agreement (for the above values of  $n$  and  $l$ ) with the predictions of formulae of FM08 and SBBW08 than with the predictions of binary spherical model given by Eq.6. The binary spherical model underestimates merger rates for small values of  $\xi$  while merger trees, for proper resolution, give results much closer to those of N-body simulations.

(iv) For large values of  $\xi$ , merger rate curves scale approximately as  $\approx \xi^{-1.5}$ .

(v) We examined steps in redshift from  $\approx 0.02$  to  $\approx 0.08$  and we found no differences in the results.

(vi) Smaller values of the resolution mass  $M_{min}$  give a better agreement with the above fitting formulae for small values of  $\xi$ .

The construction of reliable merger-trees is a subject under current investigation. These algorithms usually have fundamental problems regarding mass conservation, accurate representation of the distribution of progenitors etc. As regards N-body simulations, in addition to their resolution problems, it is characteristic that some of their results depend on the techniques used for their derivation. For example, Bett et al. (2007) showed that the values of spin parameters of haloes and their behavior as a function of mass depends crucially on the halo-finding algorithm. However, the study of physical parameters -as for example a more accurate power spectrum- seems not to be proper at this stage. Probably, the results are more sensitive to the method used for their analysis than to physical parameters and thus, any detailed description between the results of N-body and those of merger-trees may not be very useful. However, there are characteristic trends that show interesting agreement. Further improvements of tree construction algorithms as well of the quality of N-body simulations could help to understand better the physical picture during the process of the formation of dark matter haloes.

#### 5 ACKNOWLEDGEMENTS

I would like to thank the *Empirikion Foundation* for its financial support.

#### REFERENCES

- Ascasibar Y., Yepes G., Müller V., Gottlöber S., 2003, MNRAS, 346, 731  
 Bett P., Eke V., Frenk C.S., Jenkins A., Helly J., Navarro J., 2007 preprint (astro-ph/0608607v3)  
 Bond J.R., Cole S., Efstathiou G., Kaiser N., 1991, ApJ, 379, 440  
 Bond J.R., Myers S., 1996, ApJS, 103, 41  
 Cole S., 1991, ApJ, 367, 45  
 Cole S., Lacey C.G., Baugh C.M., Frenk C.S., 2000, MNRAS, 319, 168  
 Fakhouri O., Ma C-P., preprint (astro-ph/0710.4567v2) (FM08)  
 Gardner J.P., 2001, ApJ, 557, 616  
 Gelb J., Bertschinger E., 1994, ApJ, 436, 467  
 Giocoli C., Moreno J., Sheth R.K., Tormen G., 2007, MNRAS, 977-983  
 Hiotelis N., Del Popolo A., APSS, 2006, 301,167  
 Hiotelis N., 2008, APSS, 315, 191  
 Kauffmann G., White S.D.M., 1993, MNRAS, 261, 291  
 Lacey C., Cole S., 1993, MNRAS, 262, 627  
 Lacey C., Cole S., 1994, MNRAS, 271, 676  
 Lin W.P., Jing Y.P., Lin L., 2003, MNRAS, 344, 1327  
 Mahmood A., Rajesh R., 2005, preprint (astro-ph/0502513)  
 Neinstein E., Dekel A., 2008, MNRAS, 388, 1792, 2008  
 Peirani S., Mohayaee R., Pachero J., 2004, MNRAS, 348, 921  
 Press W.H., Schechter P., 1974, ApJ, 187, 425  
 Sheth R.K., Lemson G., 1999, MNRAS, 305, 946  
 Sheth R.K., Tormen G., 1999, MNRAS, 308, 119  
 Sheth R.K., Tormen G., 2002, MNRAS, 329, 61

- Smith C.C., Klypin A., Gross M.A. K., Primack J.R., Holtzman J., 1998, MNRAS, 297, 910  
Somerville R.S., Kolatt T.S., 1999, MNRAS, 305, 1  
Springel V., et al., 2005, Nat, 435, 629  
Stewart K.R., Bullock J.S., Barton E.J., Wechsler R.H., 2008, preprint (astro-ph/0811.1218v1) (SBBW08)  
Tasitsiomi A., Kratsov A.V., Gottlöbber S., Klypin A.A., 2004, ApJ, 607,125  
Vitvitska M., Klypin A.A., Kravtsov A.V., Wechsler R., Primack J., Bullock J., 2002, ApJ, 581, 799  
White S.D.M., Efstathiou G., Frenk C., 1993, MNRAS, 262, 1023  
Yahagi H., Nagashima M., Yoshii Y., 2004, ApJ, 605, 709  
Zhang J., Hui L., 2006, ApJ, 641, 641, 2005